30th International Conference
ENGINEERING MECHANICS 2024
Milovy, Czech Republic, May 14 – 16, 2024

USING FINITE VOLUME METHOD TO SIMULATE LASER SHOCK PEENING OF 7050 AL ALLOY

Isoz M.[*], **Gruber P.**[**], **Ježek O.**[***], **Kubíčková L.**[†], **Gabriel D.**[††], **Kaufman J.**[†††], **Brajer J.**[‡]

Abstract: *Laser shock peening (LSP) is a modern alternative to standard peening processes such as shot peening. In general, peening is used to improve the strength and fatigue resistance of components by hardening their surface. In LSP, a laser-induced shockwave is used to harden the material to a depth of the order of* 1 *mm, that is, roughly twice as deep as can be achieved with shot peening. Frameworks for LSP simulation have been developed since the end of the 1990s and are exclusively based on the finite element method (FEM). The critical component of the framework is the dynamic simulation of the elastoplastic shockwave that subjects the component material to a strain rate of the order* $10^{-7}\ s^{-1}$. *In this contribution, we present a simulation framework for LSP based on the finite volume method (FVM) that allows for modeling the strain-rate hardening of the material. The framework is used to simulate the LSP of the 7050 aluminum alloy. Using a comparison of our FVM results with the FEM data available in the literature, we found that FVM can be applied to LSP simulation with the same success as the more traditional FEM.*

Keywords: Laser shock peening, modeling, simulation, finite volume method, OpenFOAM.

1. Introduction

In Fig. 1, we show fundamentals of the LSP process, particularly of its water-confined variant with ablative coating applied (Scius-Bertrand et al., 2020), which is of interest in this paper. First, a high power density laser is used to convert the ablative coating (also known as the sacrificial layer) to plasma. The expanding plasma is confined by the transparent overlay and for a duration of tens of nanoseconds loads the component surface by a pressure in order of GPa. This loading generates a shockwave that propagates through the component and plasticizes its material, resulting in an affected zone with induced compressive residual stresses that are beneficiary for the fatigue resistance or surface hardness of the component.

Due to its industrial potential, attempts on numerical simulation of the laser shock peening (LSP) have been made since the end of the 1990s; see, e.g. (Braisted and Brockman, 1999; Hfaiedh et al., 2015; Sun et al., 2022). All simulations reported in the literature were performed using the finite element method (FEM). However, the critical element of the simulation appears to be the propagation of the elastoplastic shockwave. Interestingly, the finite volume method (FVM) was reported by Berezovski et al. (2014) to achieve results with no post- or pre-shock spurious oscillations for elastic wave propagation, especially when flux limiters are applied. Such a behavior is crucial for LSP simulation where spurious oscillations may lead to unphysical plastic zones and residual stresses in the material. In this contribution, we build on our previous work (Isoz et al., 2023) where we presented an FVM-based simulation framework for

[*] Ing. Martin Isoz, PhD.: Institute of Thermomechanics, Czech Academy of Sciences (CAS), Dolejškova 1402/5; 182 00, Prague; CZ, isozm@it.cas.cz

[**] Ing. Pavel Gruber, PhD.: Institute of Thermomechanics, CAS, Dolejškova 1402/5; 182 00, Prague; CZ

[***] Ing. Ondřej Ježek: Institute of Thermomechanics, CAS, Dolejškova 1402/5; 182 00, Prague; CZ

[†] Ing. Lucie Kubíčková: Institute of Thermomechanics, CAS, Dolejškova 1402/5; 182 00, Prague; CZ

[††] Ing. Dušan Gabriel, PhD.: Institute of Thermomechanics, CAS, Dolejškova 1402/5; 182 00, Prague; CZ

[†††] Ing. Jan Kaufman, PhD.: HiLASE Centre, Institute of Physics, CAS, Za Radnicí 828; 252 41, Dolní Březany; CZ

[‡] Ing. Jan Brajer, PhD.: HiLASE Centre, Institute of Physics, CAS, Za Radnicí 828; 252 41, Dolní Březany; CZ

doi: 10.21495/em2024-142

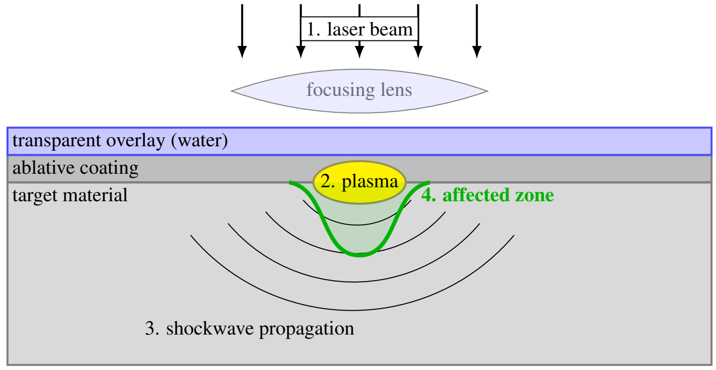

Fig. 1: Fundamentals of the laser shock peening process.

LSP implemented in the open-source C++ library OpenFOAM (OpenCFD, 2007). Here, the framework is extended by the Jonson-Cook model (Johnson and Cook, 1983) to simulate strain-rate hardening and used to recompute the study by (Sun et al., 2022), which is focused on LSP of the 7050 aluminum alloy.

2. Simulation framework fundamentals

The complete laser shock peening of the component consists of a series of individual steps, LSP shots, illustrated in Fig. 1. As stated above, the pressure loading during the shot lasts $\mathcal{O}(10^1)$ ns. Then, the shockwave looses energy required for the material plastization in $\mathcal{O}(10^3)$ ns. In-between shots, the component is repositioned, resulting in a delay of order $\mathcal{O}(10^{-1})$ s = $\mathcal{O}(10^8)$ ns. In the simulation framework, this splitting of temporal scales is reflected, in a standard manner (Braisted and Brockman, 1999; Sun et al., 2022), by simulating each shot as dynamic plastic wave propagation followed by a pseudo-static relaxation. The formal description of the process is given in (Isoz et al., 2023). Here, we will only summarize the fundamentals and focus on the new developments.

Both the dynamic and relaxation sub-steps are simulated under small-strain settings $\varepsilon = \frac{1}{2}(\nabla \boldsymbol{u} + \boldsymbol{u}\nabla)$ with damping effects and body forces neglected. The dynamic wave propagation is solved as elasto-plastic with the component internal state represented by the plastic strain ε_{p}. Newly, the plastic strain evolves under the isothermal Johnson and Cook (1983) yield criterion

$$\sigma_y = \left(A + B\varepsilon_{\mathrm{p}}^n\right)\left(1 + C\ln\left(\frac{\dot{\varepsilon}_{\mathrm{p}}}{\dot{\varepsilon}_{\mathrm{p,ref}}}\right)\right), \quad (1)$$

where $\dot{\varepsilon}_{\mathrm{p}}$ is the rate of the plastic strain, A is the static material yield strength and B, n, C are empirical parameters of which C is relevant only to the selected reference strain rate $\dot{\varepsilon}_{\mathrm{p,ref}}$. The pseudo-static relaxation is treated as perfectly elastic. However, with ε_{p} encoding the internal state of the component taken into account.

With respect to the boundary conditions used, the laser-induced loading is represented by a prescribed pressure that varies spatially and temporally. On the rest of the component surface, the boundary conditions used can correspond, for example, to the component clamping. Finally, only the surface layer of the material is directly affected by the shockwave propagation. On the other hand, residual stresses from the static sub-step reach significantly further. As a result, it is computationally profitable to solve the dynamic-sub step only in the directly affected part of the computational domain.

The problem governing partial differential equations are spatially discretized using the finite volume method as described in (Cardiff et al., 2017). The discretization schemes are usually selected to be as close as possible to second order, which is the highest global method order available in OpenFOAM (OpenCFD, 2007). Still, application of high-order schemes with flux limiting is often profitable for divergence terms. The explicit temporal integration of the shockwave propagation is performed using the standard central differencing.

3. Comparison of FVM and FEM on 7050 Al alloy

In the present contribution, our aim is to evaluate the capabilities of our FVM-based simulation framework against the state-of-the-art FEM framework. As the reference solution, the recent paper by Sun et al. (2022)

on single-shot LSP of 7050 aluminum alloy was selected, as it contains data on both the residual stresses in the material and on elasto-plastic shockwave propagation.

Simulation set-up In the FVM-based simulations, we followed the paper (Sun et al., 2022) with respect to the (i) material (7050 Al alloy), (ii) sample geometry (hexahedron of dimensions 30 × 30 × 8 mm), (iii) and spatio-temporal laser-induced pressure loading. A different computational mesh, more suitable to FVM, was used. Still, the number of degrees of freedom was approximately $1.5 \cdot 10^6$ in both the FEM and FVM simulations. Used pressure profiles and details on the material are given in Fig. 2. Comparison of the computational meshes used are shown in Fig. 3.

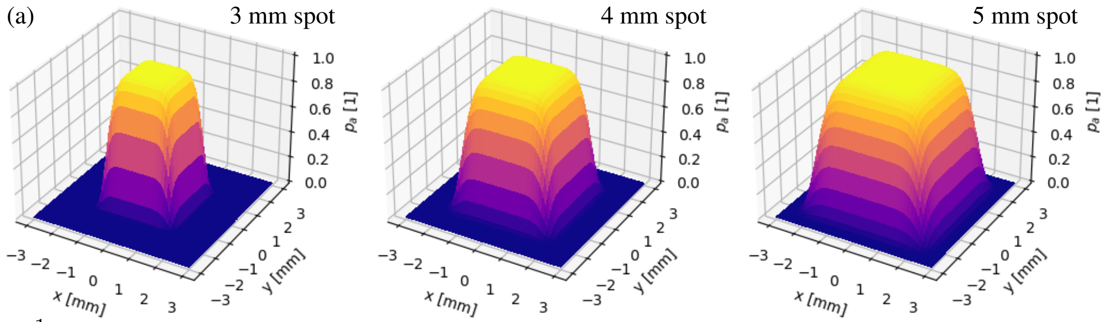

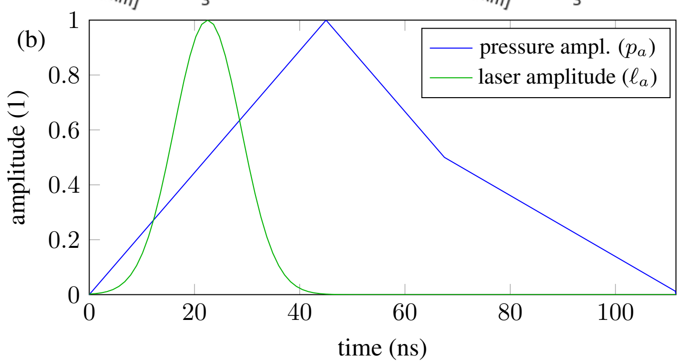

Elastic properties (c)
$\rho = 2\,800\,\mathrm{kg\,m^{-3}}$ $E = 70.3\,\mathrm{GPa}$, $\nu = 0.33$
Johnson-Cook parameters
$A = 300\,\mathrm{MPa}$, $B = 400\,\mathrm{MPa}$ $n = 0.13$, $C = 0.013$, $\dot{\varepsilon}_{\mathrm{p,ref}} = 1.0\ \mathrm{s}^{-1}$
Pressure loading
$p(t) = p_a(t)\,p_0$ p_0 from (Fabbro et al., 1990)

Fig. 2: Simulation set-up. a) spatial pressure profiles – three spot sizes were tested, b) temporal pressure and laser amplitude profiles, c) model parameters.

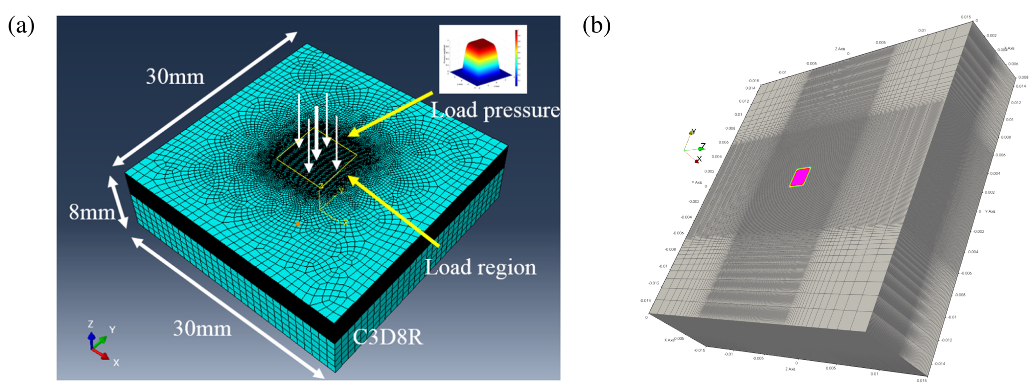

Fig. 3: Used computational meshes. a) Sun et al. (2022), b) this work.

Shockwave propagation Results for shockwave propagation at 100, 200, 400, and 600 ns and for the three spot sizes were compared with (Sun et al., 2022). In Fig. 4a, we show examples for the smallest and the biggest spots at 400 ns and 200 ns, respectively. These results were selected as they exhibit qualitatively different wave systems. However, the differences between FEM and FVM are negligible. Qualitatively different results between FEM and FVM were obtained at 600 ns. However, we contribute this difference to the fact that there is a sharp transition from a fine to a coarse mesh in FEM, see Fig. 3a. At 600 ns, the wave already passed this transition, which may have skewed the results in (Sun et al., 2022).

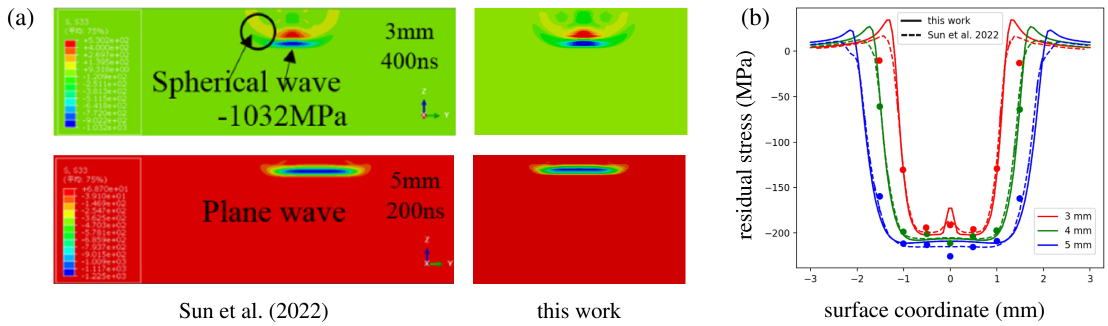

Fig. 4: Comparison of simulation results. a) shockwave propagation; same contours and same ranges are always displayed, b) residual stresses on material surface.

Residual stresses In Fig. 4b, we show a comparison of the residual stresses calculated and measured on the line on the sample surface and passing through the spot center. There are only small discrepancies between FEM and FVM while both methods agree with the experimental data rather well.

4. Conclusions

We extended our previously developed FVM-based framework for LSP simulations by the Johnson-Cook model to model the strain-rate hardening. The extended framework was used to reproduce FEM-based results of Sun et al. (2022) who dealt with simulation of a single shot LSP on 7050 aluminum alloy. It was found that both frameworks give comparable results with respect to (i) the dynamic simulation, and (ii) the final residual stresses. Future developments will be aimed at implementation of boundary conditions for pressure loading capable of mimicking those induced by imperfect industrial lasers.

Acknowledgments

The work was financially supported by the institutional support RVO:61388998 and by the grant project with No. TM04000048 of the Technology Agency of the Czech Republic.

References

Berezovski, A., Kolman, R., Blažek, J., Kopačka, J., Gabriel, D., and Plešek, J. (2014) Comparative study of finite element method, isogeometric analysis, and finite volume method in elastic wave propagation of stress discontinuities. *e-Journal of Nondestructive Testing*, 19, pp. 16321.

Braisted, W. and Brockman, R. (1999) Finite element simulation of laser shock peening. *International Journal of Fatigue*, 21, pp. 719–724.

Cardiff, P., Tukovic, Z., Jaeger, P. D., Clancy, M., and Ivankovic, A. (2017) A Lagrangian cell-centred finite volume method for metal forming simulation. *International Journal For Numerical Methods In Engineering*, 109, pp. 1777–1803.

Fabbro, R., Fournier, J., Ballard, P., Devaux, D., and Virmont, J. (1990) Physical study of laser-produced plasma in confined geometry. *Journal of Applied Physics*, 68, pp. 775–784.

Hfaiedh, N., Peyre, P., Song, H., Popa, I., Ji, V., and Vignal, V. (2015) Finite element analysis of laser shock peening of 2050-t8 aluminium alloy. *International Journal of Fatigue*, 70, pp. 480–489.

Isoz, M., Gruber, P., Schmidt, J., Kubíčková, L., Štefan, J., Kaufman, J., Brajer, J., and Gabriel, D. (2023) Calibrated finite volume method-based simulation framework for laser shock peening. In *Proc. of the Conf. Engineering Mechanics*, IT CAS, Milovy, Czech Republic, pp. 103–106.

Johnson, G. and Cook, W. (1983) A constitutive model and data for metals subjected to large strains, high strain rates, and high temperatures. In *Proc. 7th International Symposium on Ballistics*, pp. 541–547.

OpenCFD (2007) *OpenFOAM: The Open Source CFD Toolbox. User Guide Version 1.4, OpenCFD Limited.* Reading UK.

Scius-Bertrand, M., Videau, L., Rondepierre, A., Lescoute, E., Rouchausse, Y., Kaufman, J., Rostohar, D., Brajer, J., and Berthe, L. (2020) Laser induced plasma characterization in direct and water confined regimes: new advances in experimental studies and numerical modelling. *Journal of Physics D: Applied Physics*, 54, pp. 055204.

Sun, B., Zhao, J., Qiao, H., and Lu, Y. (2022) Effects of square spot size and beam quality on residual stress of 7050 aluminum alloy by laser shock peening. *Materials Chemistry and Physics*, 284, pp. 126023.